ISBN: 978-3-95450-214-1 ISSN: 2673-5490 doi:10.18429/JACoW-IPAC2021-WEXA06

# STUDY OF Pb-Pb AND Pb-p COLLISION DEBRIS IN THE CERN LHC IN VIEW OF HL-LHC OPERATION

M. Sabate-Gilarte*, R. Bruce, F. Cerutti, A. Lechner, CERN, Geneva, Switzerland

*Abstract*

For the first time, a full characterization of the Pb-Pb and Pb-p collision debris as well as its impact in terms of energy deposition in the long straight section (LSS) of CERN's Large Hadron Collider has been carried out. By means of Monte Carlo simulations with FLUKA, both inelastic nuclear interaction and electromagnetic dissociation were taken into account as source term for lead ion operation, while for Pb-p operation only nuclear interaction is of importance. The radiation exposure of detectors exclusively destined for ion beam runs is assessed, allowing drawing implications of their use in the HL-LHC era.

This work gives the opportunity for an unprecedented validation of simulation results against measurements of beam loss monitors (BLM) in the experimental LSS during ion operation. Pb-Pb operation refers to the 2018 ion run at 6.37 TeV per charge with a +160 μrad half crossing angle in the vertical plane at the ATLAS interaction point. Instead, Pb-p operation was benchmarked for the 2016 ion run at 6.5 TeV per charge with -140 μrad half crossing angle in the vertical plane at the same location.

## INTRODUCTION

Ion operation is an integral part of the LHC and HL-LHC (Run 4) programs [1–3]. Despite the significantly lower beam intensity and luminosity with respect to proton operation, it poses relevant challenges in terms of machine protection, due to the specific interaction processes it features. Apart from the much worse cleaning efficiency provided by the collimation system when dealing with lead beams compared to the proton case, due to the yield of off-momentum heavy-ion fragments produced in the primary collimators and impacting the superconducting magnets in the Dispersion Suppressor (DS) [4, 5], the experimental insertions are subject to the localised impact of the secondary $^{208}Pb^{81+}$ beam generated at the Interaction Point (IP) by Bound-Free Pair Production (BFPP), as the electron generated by the ion electromagnetic interaction is captured by one of the colliding nuclei. This issue has been anticipated long ago [6–8] and was recently discussed in detail based on the actual LHC experience [9]. Here we rather focus on the radiation impact on the Long Straight Section (LSS) of the ATLAS insertion, to a good extent representative of the CMS one too, and for this purpose we consider as source term both inelastic nuclear interactions (INI), simulated by the DPMJET-3 [10, 11] event generator interfaced to FLUKA [12–14], and ion electromagnetic dissociation (EMD). The latter process, whose description is fully integrated in FLUKA [15], implies a virtual photon exchange and the excitation of one of the colliding nuclei, which consequently emits some nucleons, mostly one or two neutrons, and so generates a residual nucleus typically close, in mass and charge, to the original ion. For proton-lead collisions, only the INI term has to be taken into account, since all electromagnetic cross sections are strongly suppressed by the low proton charge.

* marta.sabate.gilarte@cern.ch

## HEAVY ION COLLISIONS AT THE LHC

This paper reports studies referring both to the Pb-Pb and Pb-p operation modes in the Run 2 of the present LHC machine, as well as Pb-Pb calculations for the future HL-LHC configuration during Run 4.

### *Pb-Pb Run*

The actual conditions of the 2018 LHC Pb-Pb run [16] have been simulated, with a half crossing angle of +160 μrad in the vertical plane at IP1 (center of the ATLAS detector) and a beam energy of 6.37 TeV per charge, i.e. 522 TeV per interacting ion, equivalent to a nucleon-nucleon centre-of-mass energy of $\sqrt{s_{NN}} = 5.02$ TeV. The physics debris collimators (TCL) were open during this run. As mentioned above, independent FLUKA simulations of the particle shower propagation in the LSS on the right side of ATLAS were performed for INI and EMD events and normalized to the respective cross sections, namely 7.8 b and 430 b (the latter value refers to the EMD of either of the two interacting ions) as obtained by FLUKA.

Figure 1 highlights the varying weight of the two contributions as a function of the distance from the collision point, with the INI debris dominating in the close region of the final focus quadrupoles (triplet) and further surpassed by the impact of EMD fragments, although only 5% of their energy is deposited in the LSS. For an instantaneous luminosity of $10^{27}$ cm$^{-2}$ s$^{-1}$, the total power deposited in the triplet cold masses amounts to 34 mW, which is more than three orders of magnitude lower than the load experienced during proton operation [17] and indicates that the induced power density and integrated dose in the superconducting coils is negligible.

### *Pb-p Run*

During the LHC Run 2, a Pb-p run was also performed. Because of its intrinsic asymmetry, we simulated it assuming as outgoing beam on the right side of the ATLAS LSS either the lead and proton beam, and the results are referred to as *Pb-side* and *p-side*, respectively. According to the Pb-p run configuration in 2016 [18, 19], a half crossing angle of -140 μrad was implemented in the vertical plane at IP1, corresponding to colliding beams pointing downwards. The considered beam energy is 6.5 Z TeV, yielding a nucleon-nucleon centre-of-mass energy of $\sqrt{s_{NN}} = 8.16$ TeV. The TCL

Content from this work may be used under the terms of the CC BY 3.0 licence (© 2021). Any distribution of this work must maintain attribution to the author(s), title of the work, publisher, and DOI

12th Int. Particle Acc. Conf. IPAC2021, Campinas, SP, Brazil JACoW Publishing
ISBN: 978-3-95450-214-1 ISSN: 2673-5490 doi:10.18429/JACoW-IPAC2021-WEXA06

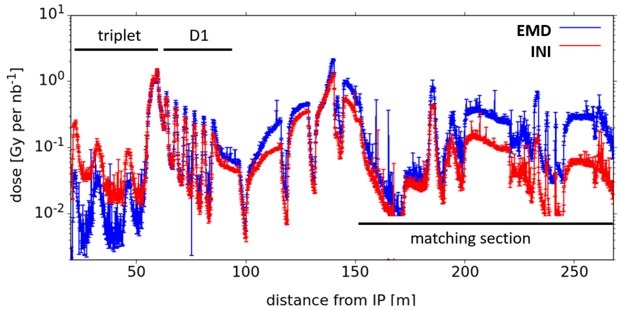


Figure 1: Dose profile below the beam line along the LSS on the right of IP1 as induced by Pb-Pb collisions. Values are averaged over a 40 cm horizontal interval centred on the machine axis and a 20 cm vertical interval centred 60 cm below the machine axis. They are normalized to a reference integrated luminosity of 1 nb$^{-1}$. INI and EMD contributions are shown separately.

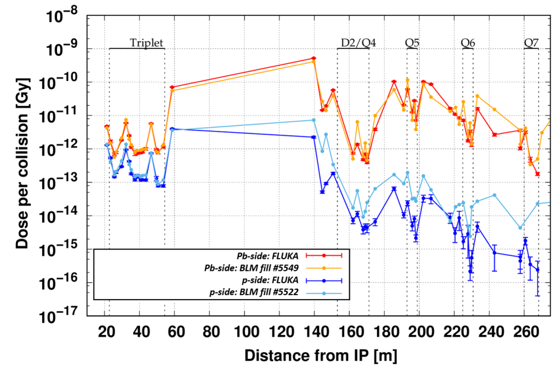


Figure 3: BLM pattern along the LSS on the right side of IP1, as measured during the indicated Pb-p (orange) and p-Pb (light blue) physics fills and simulated with FLUKA (red and blue, respectively). Experimental doses are divided by the product of the fill luminosity and the 2.11 b INI cross section value.

collimators were kept open again. Here the source term is exclusively represented by the products of INI events, for which a cross section of 2.11 b is used as given by FLUKA. The instantaneous luminosity approached $10^{30}$ cm$^{-2}$ s$^{-1}$, more than two orders of magnitudes higher than in Pb-Pb.

Figure 2 presents the peak dose profile in the inner coils of the different triplet magnets for both sides (obtained by swapping the beam directions). While the values remain negligible in absolute terms, one can appreciate the one order of magnitude separation between the two sides, still not entirely reflecting the beam energy difference in favour of lead ions (carrying an energy 82 times higher). Such a discrepancy applies to this portion of the machine, mostly impacted by charged mesons captured by the quadrupole fields, whereas the gap between the two sides rises to the expected level further downstream (as indicated by Fig. 3), at the position of the TAN absorber that takes a good fraction of the debris energy where the interaction region vacuum tube splits in two distinct chambers.

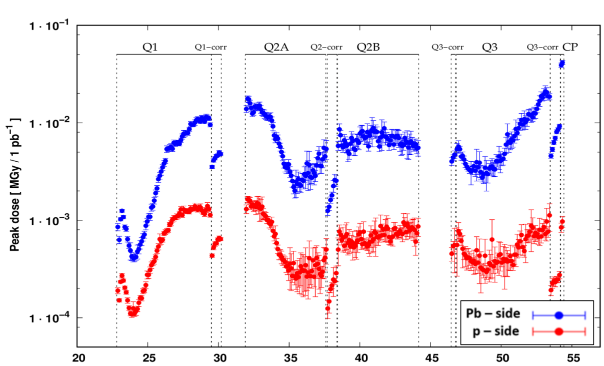


Figure 2: Peak dose profile in the inner coils of the triplet as a function of the distance from the IP, induced by Pb-p collisions on the *Pb-side* (blue) and the *p-side* (red). Values are normalized to a reference integrated luminosity of 1 pb$^{-1}$.

## BLM BENCHMARKING

Beam Loss Monitors (BLM) [20, 21] are gaseous detectors installed all along the LHC ring in the proximity of the beam line with the purpose of providing an on-line dose measurement during operation and triggering a beam abort if pre-defined limits are exceeded, as an evidence of abnormal losses. A detailed BLM model is also implemented in FLUKA in order to calculate the dose deposited in the gas volume of any monitor for the simulated loss scenario, such as the one of regular collisions. This already allowed an extensive validation of FLUKA predictions regarding the LHC [22], which we complement with the unprecedented evaluations of this paper.

In fact, Fig. 4 displays a quite satisfactory absolute agreement for the Pb-Pb case, apart from the factor 2 overestimation at the TAN BLM, at 140 m from the IP, deserving further investigations. On the other hand, in Fig. 3 the matching between data and simulations is remarkable on the *Pb-side*, except for the local underestimation behind the Q6 quadrupole, and remains excellent on the *p-side* as far as the triplet is concerned. In the latter case, while the low readings beyond 140 m are affected by an important systematic uncertainty related to the background subtraction, the clear underestimation at the TAN calls also for additional verifications.

## Pb-Pb COLLISIONS AT THE HL-LHC

The upgrade of the LHC, aimed to reach significantly higher luminosities [2, 3], implies the substantial renovation of the ATLAS and CMS insertions. In this context, a dedicated study has been carried out to characterize the radiation environment to be faced by the detectors accommodated in the new TAXN neutral absorber during ion operation. These are the Zero Degree Calorimeter (ZDC), which is removed during proton runs, and the Beam RAte of Neutral (BRAN) [23]. The latest version of the machine layout was

Content from this work may be used under the terms of the CC BY 3.0 licence (© 2021). Any distribution of this work must maintain attribution to the author(s), title of the work, publisher, and DOI

ISBN: 978-3-95450-214-1 ISSN: 2673-5490 doi:10.18429/JACoW-IPAC2021-WEXA06

Content from this work may be used under the terms of the CC BY 3.0 licence (© 2021). Any distribution of this work must maintain attribution to the author(s), title of the work, publisher, and DOI

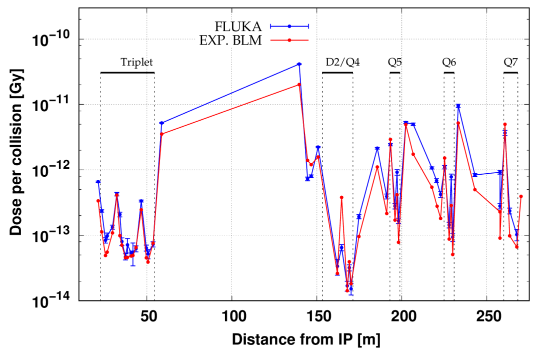


Figure 4: BLM pattern along the LSS on the right side of IP1, as measured during the Pb-Pb physics fill #7473 in 2018 and simulated with FLUKA. Experimental doses are divided by the product of the fill luminosity and the 438 b cross section value, corresponding to the sum of the INI and EMD cross sections.

implemented in FLUKA for protons simulations with the optics v1.5 [24] and used also for assessing the impact of Pb-Pb collisions in IP1. These refer to 7 TeV per charge lead beams, i.e. $\sqrt{s_{NN}} = 5.52$ TeV, crossing in the vertical plane with a half angle of +170 µrad. We considered once more INI and EMD events, weighted by a cross section of 7.8 b and 450 b, respectively.

Figure 5 presents the peak dose profile in the inner coils of the present and new superconducting magnet string adjacent to the ATLAS cavern. The comparison highlights the effectiveness of the HL-LHC design, where the more than doubled magnet aperture and the massive tungsten shielding incorporated on the beam screen of the final focusing magnets imply a very important reduction of the coil exposure, such as to cope with the luminosity increase planned for proton operation (the cumulated contribution of ion runs is here negligible). At the envisaged instantaneous luminosity of $6{\cdot}10^{27}$ cm$^{-2}$ s$^{-1}$, the total power deposited over the HL-LHC Q1-D1 magnets amounts to 560 mW.

The radiation environment generated in the LSS by lead beam collisions, albeit much less severe than in proton runs, is still relevant for the equipment specific to ion operation. In particular, the risk of failure for the modules of readout electronics linked to the ZDC has to be evaluated as a function of the expected levels of high energy hadron fluence (HEH), thermal neutron fluence and total ionizing dose (TID) in the region of interest. Figure 6 shows the resulting annual HEH fluence profile along the LSS for the LHC and HL-LHC machines, where the peak closest to the IP corresponds in both cases to the location of the neutral absorber (TAN and TAXN, respectively). The different structure of the two curves reflects the machine layout changes.

## CONCLUSION

The calculation of Pb-Pb and Pb-p collision losses in a LHC experimental insertion was carried out with FLUKA, quantifying the particle shower impact on the different accelerator elements and providing the first simulation benchmarking of this source term against extended LSS BLM data at IR1. This provides a basis for further studies in support of future ion operation. In this perspective, the lead beam case was investigated in the HL-LHC scenario to assess the radiation levels relevant to the instrumentation specific to ion runs.

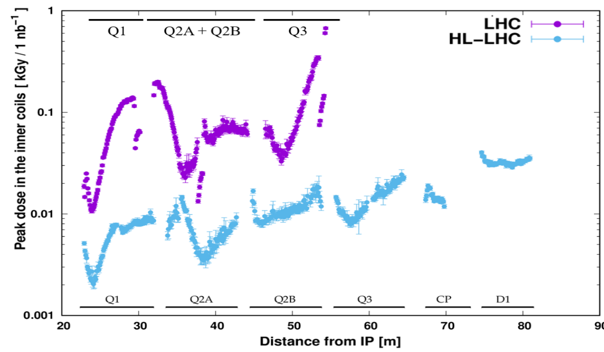


Figure 5: Peak dose profile in the inner coils of the LHC Q1-Q3 string (purple) and HL-LHC Q1-D1 string (blue), as induced by INI and EMD events in Pb-Pb collisions. For the purpose of comparison, values are normalised in both cases to a reference integrated luminosity of 1 nb$^{-1}$.

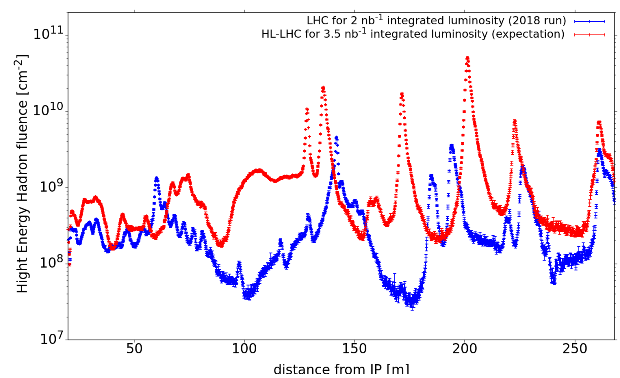


Figure 6: High energy hadron fluence profile along the LSS on the right of IP1 as induced by Pb-Pb collisions in the HL-LHC (red) and LHC (blue) configuration. Values averaged over a 40 cm horizontal interval centred on the machine axis and a 20 cm vertical interval centred 30 cm from the floor level. They are normalized to an annual integrated luminosity of 3.5 nb$^{-1}$ and 2 nb$^{-1}$, respectively. INI and EMD contributions are added up according to their cross sections.

## ACKNOWLEDGEMENTS

The authors would like to thank J. Jowett, R. De Maria and M. Schaumann for their valuable input regarding the LHC ion operation parameters and enlightening discussions. Research supported by the HL-LHC project.

ISBN: 978-3-95450-214-1 ISSN: 2673-5490 doi:10.18429/JACoW-IPAC2021-WEXA06

## REFERENCES

[1] O. S. Brüning *et al.*, "LHC Design Report", CERN, Geneva, Switzerland, Rep. CERN-2004-003-V-1, 2004.

[2] I. Béjar Alonso *et al.*, "High-Luminosity Large Hadron Collider (HL-LHC): Technical Design Report", CERN, Geneva, Switzerland, Rep. CERN-2020-010, 2020.

[3] R. Bruce *et al.*, "HL-LHC operational scenario for Pb-Pb and p-Pb operation", CERN, Geneva, Switzerland, Rep. CERN-ACC-2020-0011, Jul. 2020.

[4] P. D. Hermes *et al.*, "Measured and simulated heavy-ion beam loss patterns at the CERN Large Hadron Collider", *Nuclear Instruments and Methods in Physics Research Section A: Accelerators, Spectrometers, Detectors and Associated Equipment*, vol. 819, pp. 73–83, May 2016. doi:10.1016/j.nima.2016.02.050

[5] N. Fuster-Martínez *et al.*, "Simulations of heavy-ion halo collimation at the CERN Large Hadron Collider: Benchmark with measurements and cleaning performance evaluation", *Physical Review Accelerators and Beams*, vol. 23, no. 11, p. 111002, Nov. 2020. doi:10.1103/physrevaccelbeams.23.111002

[6] S. R. Klein, "Localized beampipe heating due to e- capture and nuclear excitation in heavy ion colliders", *Nuclear Instruments and Methods in Physics Research Section A: Accelerators, Spectrometers, Detectors and Associated Equipment*, vol. 459, no. 1–2, pp. 51–57, Feb. 2001. doi:10.1016/s0168-9002(00)00995-5

[7] R. Bruce *et al.*, "Observations of Beam Losses Due to Bound-Free Pair Production in a Heavy-Ion Collider", *Physical Review Letters*; vol. 99, no. 14, p. 144801, Oct. 2007. doi:10.1103/PhysRevLett.99.144801

[8] R. Bruce, S. S. Gilardoni, and J. M. Jowett, "Effects of Ultraperipheral Nuclear Collisions in the LHC and their Alleviation", in *Proc. 11th European Particle Accelerator Conf. (EPAC'08)*, Genoa, Italy, Jun. 2008, paper WEPP006, pp. 2533-2535.

[9] M. Schaumann, J. M. Jowett, C. Bahamonde Castro, R. Bruce, A. Lechner, and T. Mertens, "Bound-free pair production from nuclear collisions and the steady-state quench limit of the main dipole magnets of the CERN Large Hadron Collider", *Physical Review Accelerators and Beams*, vol. 23, no. 12, p. 121003, Dec. 2020. doi:10.1103/physrevaccelbeams.23.121003

[10] S. Roesler, R. Engel, and J. Ranft, "The Monte Carlo Event Generator DPMJET-III", in *Proc. Int. Conf. on Advanced Monte Carlo for Radiation Physics, Particle Transport Simulation and Applications*, Lisbon, Oct. 2000, pp. 1033-1038. Springer-Verlag Berlin, 1033-1038 (2001).

[11] A. Fedynitch, "Cascade equations and hadronic interactions at very high energies", Ph.D. thesis, Karlsruhe Institute of Technology, Karlsruhe, Germany, 2015.

[12] FLUKA, https://fluka.cern

[13] G. Battistoni *et al.*, "Overview of the FLUKA code", *Annals of Nuclear Energy*, vol. 82, pp. 10-18, Aug. 2015. doi:10.1016/j.anucene.2014.11.007

[14] T. T. Bohlen *et al.*, "The FLUKA Code: Developments and Challenges for High Energy and Medical Applications", *Nuclear Data Sheets*, vol. 120, pp. 211-214, Jun. 2014. doi:10.1016/j.nds.2014.07.049

[15] H. H. Braun, A. Fassò, A. Ferrari, J. M. Jowett, P. R. Sala, and G. I. Smirnov, "Hadronic and electromagnetic fragmentation of ultrarelativistic heavy ions at LHC", *Physical Review Special Topics - Accelerators and Beams*, vol. 17, no. 2, p. 021006, Feb. 2014. doi:10.1103/physrevstab.17.021006

[16] J. M. Jowett *et al.*, "The 2018 Heavy-Ion Run of the LHC", in *Proc. 10th Int. Particle Accelerator Conf. (IPAC'19)*, Melbourne, Australia, May 2019, pp. 2258-2261. doi:10.18429/JACoW-IPAC2019-WEYYPLM2

[17] C. Hoa, F. Cerutti, and E. Wildner, "Energy Deposition in the LHC Insertion Regions IR1 and IR5", CERN, Geneva, Switzerland, Rep. LHC-PROJECT-Report-1167, Sep. 2008.

[18] J. M. Jowett *et al.*, "The 2016 Proton-Nucleus Run of the LHC", in *Proc. 8th Int. Particle Accelerator Conf. (IPAC'17)*, Copenhagen, Denmark, May 2017, pp. 2071-2074. doi:10.18429/JACoW-IPAC2017-TUPVA014

[19] M. A. Jebramcik, "Beam Dynamics of Proton-Nucleus Collisions in the Large Hadron Collider", Ph.D. thesis, Goethe University Frankfurt, Frankfurt, Germany, 2020.

[20] E. B. Holzer *et al.*, "Beam loss monitoring system for the LHC", in *IEEE Nuclear Science Symposium Conf. Record*, Fajardo, PR, USA, Oct. 2005, pp. 1052-1056. doi:10.1109/NSSMIC.2005.1596433

[21] E. B. Holzer *et al.*, "Development, Production and Testing of 4500 Beam Loss Monitors", in *Proc. 11th European Particle Accelerator Conf. (EPAC'08)*, Genoa, Italy, Jun. 2008, paper TUPC037, pp. 1134-1136.

[22] A. Lechner *et al.*, "Validation of energy deposition simulations for proton and heavy ion losses in the CERN Large Hadron Collider", *Physical Review Accelerators and Beams*, vol. 22, no. 7, p. 071003, Jul. 2019. doi:10.1103/PhysRevAccelBeams.22.071003

[23] H. S. Matis *et al.*, "The BRAN luminosity detectors for the LHC", *Nuclear Instruments and Methods in Physics Research Section A: Accelerators, Spectrometers, Detectors and Associated Equipment*, vol. 848, pp. 114-126, Mar. 2017. doi:10.1016/j.nima.2016.12.019

[24] M. Sabate-Gilarte and F. Cerutti, "Energy Deposition Study of the CERN HL-LHC Optics v1.5 in the ATLAS and CMS Insertions", presented at the 12th Int. Particle Accelerator Conf. (IPAC'21), Campinas, Brazil, May 2021, paper MOPAB012, this conference.

Content from this work may be used under the terms of the CC BY 3.0 licence (© 2021). Any distribution of this work must maintain attribution to the author(s), title of the work, publisher, and DOI